THE JOURNAL OF BIOLOGICAL CHEMISTRY VOL. 291, NO. 2, pp. 752–761, January 8, 2016

Regulation of c-Myc Expression by Ahnak Promotes Induced Pluripotent Stem Cell Generation*

Received for publication, April 15, 2015, and in revised form, November 18, 2015 Published, JBC Papers in Press, November 23, 2015, DOI 10.1074/jbc.M115.659276

Hee Jung Lim[‡], Jusong Kim[‡], Chang-Hwan Park[§], Sang A. Lee[¶], Man Ryul Lee[¶], Kye-Seong Kim[§], Jaesang Kim[‡1], and Yun Soo Bae[‡2]

From the [‡]Department of Life Sciences, Ewha Womans University, Seoul 120-750, Korea, the [§]Graduate School of Biomedical Science and Engineering, Department of Biomedical Science, Hanyang University, Seoul 133-791, Korea, and the [¶]Soonchunhyang Institute of Medi-bioscience, Soon Chun Hyang University, Cheonan 31538, Korea

We have previously reported that Ahnak-mediated TGFβ signaling leads to down-regulation of c-Myc expression. Here, we show that inhibition of Ahnak can promote generation of induced pluripotent stem cells (iPSC) via up-regulation of endogenous c-Myc. Consistent with the c-Myc inhibitory role of Ahnak, mouse embryonic fibroblasts from Ahnak-deficient mouse (Ahnak$^{-/-}$ MEF) show an increased level of c-Myc expression compared with wild type MEF. Generation of iPSC with just three of the four Yamanaka factors, Oct4, Sox2, and Klf4 (hereafter 3F), was significantly enhanced in Ahnak$^{-/-}$ MEF. Similar results were obtained when Ahnak-specific shRNA was applied to wild type MEF. Of note, expression of Ahnak was significantly induced during the formation of embryoid bodies from embryonic stem cells, suggesting that Ahnak-mediated c-Myc inhibition is involved in embryoid body formation and the initial differentiation of pluripotent stem cells. The iPSC from 3F-infected Ahnak$^{-/-}$ MEF cells (Ahnak$^{-/-}$-iPSC-3F) showed expression of all stem cell markers examined and the capability to form three primary germ layers. Moreover, injection of Ahnak$^{-/-}$-iPSC-3F into athymic nude mice led to development of teratoma containing tissues from all three primary germ layers, indicating that iPSC from Ahnak$^{-/-}$ MEF are *bona fide* pluripotent stem cells. Taken together, these data provide evidence for a new role for Ahnak in cell fate determination during development and suggest that manipulation of Ahnak and the associated signaling pathway may provide a means to regulate iPSC generation.

It has been well established that the so-called Yamanaka factors, Oct4 (octamer-binding transcription factor 4), Sox2 (SRY (sex determining region Y)-box 2), Klf4 (Kruppel-like factor 4), and c-Myc, together stimulate the generation of induced pluripotent stem cells (iPSC)[3] from diverse types of somatic cells including embryonic fibroblast cells (1–5). Oct4 belongs to the family of POU transcriptional factors and binds to an octamer sequence motif, AGTCAAAT, leading to expression of target genes in developing germ cells (6, 7). Sox2 is a member of Sox transcriptional factor family containing the high mobility group domain and is known to be required for maintenance of diverse types of stem cells throughout life (8). KLF4 is a member of Kruppel-like factor transcriptional factor family that binds to CACCC sequence regulating gene expression during embryonic development (9, 10). c-Myc is a well known basic helix-loop-helix transcriptional factor that plays important roles in cell cycle regulation, cellular transformation, and maintenance of pluripotency (11, 12).

Ahnak is an exceptionally large protein (~700 kDa) and has an extended central region composed of 36 repeat units that serve as a scaffolding motif for interaction of phospholipase C-γ with PKC in regulation of cell proliferation and migration (13–16). Moreover, the central repeated unit is known to bind to R-Smad protein in response to TGF-β and mediate down-regulation of c-Myc expression and cell growth retardation. Specifically, nuclear localization of Ahnak in complex with phospho-Smad3 and binding to promoter of *c-Myc* were strongly enhanced in response to TGF-β, indicating that Ahnak down-regulates the expression of c-Myc as Smad3 target genes. Consistently, Ahnak-deficient MEF cells show a significant up-regulation of c-Myc expression (17).

There have been efforts to exclude c-Myc from the mix of ectopically expressed transcription factors for iPSC generation mainly because of its potential transforming activity. Exclusion of c-Myc, however, led to a dramatic reduction in efficiency (18–20). Therefore, developing a method to efficiently utilize endogenous c-Myc activity for iPSC generation could represent an important progress. Here, we present that Ahnak knock-out MEF or wild type MEF expressing shRNA specific to Ahnak can be converted to iPSC at a high efficiency without infection of c-Myc retrovirus. Further dissection of Ahnak pathway may provide novel strategies for regulation of iPSC generation and reducing the potential danger from cellular transformation.

* This work was supported by National Research Foundation of Korea Grant 2012R1A5A1048236, by Bio & Medical Technology Development Program Grant 2012M3A9B4028785, Redoxomics Grant 2012M3A9C5048708 funded by the Ministry of Science, ICT & Future Planning. This work was also supported by Grant A120262 from the Ministry of Health & Welfare, Republic of Korea. The authors declare that they have no conflicts of interest with the contents of this article.

[1] To whom correspondence may be addressed: Dept. of Life Sciences, Ewha Womans University, Daehyun-Dong, Seodaemoon-Gu, Seoul 120-750, Korea. Tel.: 82-2-3277-3414; Fax: 82-2-3277-3760; E-mail: jkim1964@ewha.ac.kr.

[2] To whom correspondence may be addressed: Dept. of Life Sciences, Ewha Womans University, Daehyun-Dong, Seodaemoon-Gu, Seoul 120-750, Korea. Tel.: 82-2-3277-2729; Fax: 82-2-3277-3760; E-mail: baeys@ewha.ac.kr.

[3] The abbreviations used are: iPSC, induced pluripotent stem cell(s); MEF, mouse embryonic fibroblast(s); AP, alkaline phosphatase; EB, embryoid body; ES, embryonic stem; HFF, human foreskin fibroblast; OSK, Oct4, Sox2, and Klf4; OSKM, Oct4, Sox2, Klf4, and c-Myc.

Materials and Methods

Isolation of Mouse Embryonic Fibroblasts—MEF were isolated from embryos at embryonic day 13.5. The uterus was dissected out from each mouse and rinsed with PBS. After isolation of each fetus, the head and internal organs were removed to isolate only the trunk, which was subsequently finely minced by ejection through a 10-ml syringe. The mixture of cells and small tissue masses was incubated with 5 ml of trypsin-EDTA at 37 °C with shaking for 30 min. Digestion was terminated with addition of FBS, and cells were resuspended in fresh medium (DMEM, 10% FBS) and transferred to 150-mm culture dishes. The MEF were grown to 70–80% confluence prior to passage. MEF from two- or four-passage cultures were used in all experiments.

Cell Cultures—MEF and human foreskin fibroblasts (HFF; ATCC, Manassas, VA) cells were cultured at 37 °C in an atmosphere of 5% CO_2 in DMEM supplemented with 10% FBS and 1% antibiotic-antimycotic solution (Welgene, Daegu, Korea). CF1 MEF feeder cells were cultured in DMEM supplemented with 10% FBS, 0.1 mM MEM nonessential amino acid (Invitrogen, Waltham, MA), 2 mM GlutaMAX (Gibco), 100 units/100 μg/ml penicillin/streptomycin (Gibco), and 0.1 mM β-mercaptoethanol (Gibco). J1 mouse ES cells (ATCC) and iPSC were maintained on mitomycin C-treated MEF feeder cells (CF1 strain) in DMEM supplemented with 15% FBS, 0.1 mM MEM nonessential amino acid (Invitrogen), 2 mM GlutaMAX (Gibco), 1 mM sodium pyruvate (Gibco), 100 units/100 μg/ml penicillin/streptomycin (Gibco), 0.1 mM β-mercaptoethanol (Gibco), and 1000 units/ml leukemia inhibitory factor (Millipore, Billerica, MA). For production of retroviruses, 293GPG packaging cells were maintained in DMEM containing 10% FBS, 0.1 mM MEM nonessential amino acid (Invitrogen), 2 mM GlutaMAX (Gibco), 100 units/100 μg/ml penicillin/streptomycin (Gibco), 10 mM HEPES buffer, 8 mM NaOH, 2 μg/ml tetracycline (Sigma), 2 μg/ml puromycin (Sigma), and 300 μg/ml of geneticin (Gibco).

Production of Retrovirus Encoding OCT4, SOX2, KLF4, or c-Myc—The pMXs-IRES-Puro-based retroviral expression vectors for mouse OCT4, SOX2, KLF4, and c-Myc were obtained from Addgene (Cambridge, MA). For knockdown of Ahnak in mouse and human cells, an shRNA targeting Ahnak in a microRNA scaffold (miR-shRNA) was utilized (21). A long duplex oligonucleotide containing an Ahnak targeting sequence, 5′-ATCTCCATGCCTGATGTGG-3′, within the mir-30 context was synthesized in pGEM-T Easy cloning vector (Bioneer Inc., Daejeon, Korea). To target human Ahnak for the control, a scrambled sequence was utilized. The construct was ligated 5′ to IRES-GFP in LZRS retroviral vector as previously described.

The day before transduction, 293GPG packaging cells were seeded at 6×10^6 cells per T-75 flask. Retroviral vectors were transfected using Lipofectamine 2000 (Invitrogen) according to the manufacturer's protocol. After transfection, cells were selected using 2 μg/ml tetracycline (Sigma), 10 μg/ml puromycin (Sigma), and 300 μg/ml of geneticin (Gibco). After growth with selection, DMEM without antibiotics were applied to cells to induce production of retroviruses. Virus-containing supernatants derived from these 293GPG cell cultures were filtered through a 0.45-μm syringe filter (Pall Corporation, Port Washington, NY) and supplemented with 4 μg/ml Polybrene (Sigma). Target MEF were seeded at 1.5×10^5 cells per 35-mm dish 24 h prior to infection and treated twice with the virus/Polybrene-containing supernatants for 24 h. The cells were subsequently cultured in mouse ES medium (DMEM supplemented with 15% FBS, 0.1 mM MEM nonessential amino acid (Invitrogen), 2 mM GlutaMAX (Gibco), 1 mM sodium pyruvate (Gibco), 100 units/100 μg/ml penicillin/streptomycin (Gibco), 0.1 mM β-mercaptoethanol (Gibco) containing leukemia inhibitory factor (Millipore). Puromycin at a final concentration of 1.5 μg/ml for selection was applied to transduced cells. Colonies were AP-stained (see below) and counted for comparative quantitation 18 days after viral transduction. Some colonies were also isolated from the culture for expansion. Clones WT-iPSC-4F-19, WT-iPSC-3F-6, Ahnak$^{-/-}$-iPSC-4F-31, and Ahnak$^{-/-}$-iPSC-3F-8 were used for detailed characterization.

HFF derived iPSC were generated by three factors (OSK) in combination with retrovirus encoding scrambled control shRNA or Ahnak-specific shRNA. HFF cells were cultured in DMEM containing 10% FBS. At day 2, about 5×10^5 cells were infected with concentrated viral preparations with 8 μg/ml Polybrene (Sigma-Aldrich). The next day, the medium was replaced with fresh medium and cultured for another 3 days. At the end of day 5, cells were transferred to mitotically inactivated MEF. Cells were subsequently cultured in DMEM containing 10% FBS for another 2 days, and the medium was replaced with human ES cell medium (DMEM-F12 with 20% KOSR (KnockOut Serum Replacement, Gibco). Colonies were AP-stained and counted 14 days after the viral transduction.

Alkaline Phosphatase (AP) Staining—To detect AP activity, the cells were washed with PBS, fixed with 4% paraformaldehyde in PBS for 10 min at room temperature and washed with distilled water. They were stained with 5-bromo-4-chloro-3-indolyl-phosphate/nitro blue tetrazolium color development substrate kit (Promega, Fitchburg, WI) according to the manufacturer's protocol. The stained cells were photographed, and the colonies were counted.

Embryoid Body (EB) Formation and in Vitro Differentiation—J1 mouse ES or iPSC colonies were harvested by trypsinization and suspended in mouse ES medium without leukemia inhibitory factor. The single cells were cultured in suspension in untreated Petri dishes to generate embryoid bodies. After 7 days, aggregated cells were plated onto gelatin-coated coverslips in 12-well plates and incubated for another 14 days. The cells were stained with anti-βIII-tubulin (Millipore), anti-smooth muscle actin (clone 1A4; Dako, Glostrup, Denmark), and anti-α-fetoprotein (Dako).

Immunofluorescence Staining—J1 mouse ES cells and iPSC were plated in 12-well plates on coverslips. Cells were fixed with 4% paraformaldehyde in PBS for 10 min at room temperature, washed with PBS, and then permeabilized in 0.5% Triton X-100 for 10 min. After blocking with PBS containing 1% bovine serum albumin for 1 h at room temperature, the cells were incubated with primary antibodies against anti-Oct4 (H-134; Santa Cruz Biotechnology, Santa Cruz, CA), anti-Sox2 (Millipore), and anti-stage-specific embryonic antigen 1 (SSEA1;

Santa Cruz Biotechnology) in PBS overnight at 4 °C. After washing three times with PBS and incubating with the secondary antibodies, rhodamine-conjugated goat anti-mouse IgG (KPL, Gaithersburg, MD), or Alexa Fluor® 594-conjugated goat anti-rabbit IgG (Life Technologies, Inc.) for 1 h at room temperature in the dark, cells were counterstained with DAPI cells and examined with a LSM510 meta confocal laser scanning microscope (Carl Zeiss, Oberkochen, Germany).

RNA Extraction and Quantitative Real Time PCR—Total RNA was prepared with TRIzol reagent (Molecular Research Center, Inc., Cincinnati, OH) following the manufacturer's protocol. cDNA was synthesized using 1 μg of RNA/20 μl of reaction volume with GoScript^{TM} reverse transcription system (Promega). Quantitative PCR analysis was performed in duplicate using an Applied Biosystems (Foster City, CA) model 7300 instrument with TaqMan® PCR master mix (Kapa Biosystems, Wilmington, MA) or SYBR® Green PCR master mix (Kapa Biosystems) according to the manufacturers' protocols. Predesigned, gene specific TaqMan® mouse Ahnak and GAPDH probe were purchased from Applied Biosystems. The relative quantitation of gene expression was obtained using the comparative CT method, and the results were normalized against GAPDH or 18S rRNA as the endogenous control. The following oligonucleotide primers were used in PCR: total OCT4 F, 5′-CTGAGGGCCAGGCAGGAGCACGAG-3′; total OCT4 R, 5′-CTGTAGGGAGGGCTTCGGGCACTT-3′; endogenous OCT4 F, 5′-TAGGTGAGCCGTCTTTCCAC-3′; endogenous OCT4 R, 5′-GCTTAGCCAGGTTCGAGGAT-3′; total SOX2 F, 5′-GGTTACCTCTTCCTCCCACTCCAG-3′; total SOX2 R, 5′-TCACATGTGCGACAGGGGCAG-3′; endogenous SOX2 F, 5′-TTAACGCAAAAACCGTGATG-3′; endogenous SOX2 R, 5′-GAAGCGCCTAACGTACCACT-3′; total KLF4 F, 5′-CACCATGGACCCGGGCGTGGCTGCCA-3′; total KLF4 R, 5′-TTAGGCTGTTCTTTTCCGGGGCCACGA-3′; endogenous KLF4 F, 5′-GCGAACTCACACAGGCGAGAAACC-3′; endogenous KLF4 R, 5′-TCGCTTCCTCTTCCTCCGACACA-3′; total c-Myc F, 5′-TCTCCACTCACCAGCACAACTACG-3′; total c-Myc R, 5′-ATCTGCTTCAGGACCCT-3′; endogenous c-Myc F, 5′-TGACCTAACTCGAGGAGGAGCTGGAATC-3′; endogenous c-Myc R, 5′-AAGTTTGAGGCAGTTAAAATTATGGCTGAAGC-3′; FGF5 F, 5′-TGTACTGCAGAGTGGGCATC-3′; FGF5 R, 5′-ACAATCCCCTGAGACACAGC-3′; Nestin F, 5′-CCCTGAAGTCGAGGAGCTG-3′; Nestin R, 5′-CTGCTGCACCTCTAAGCGA-3′; Eomes F, 5′-GCGCATGTTTCCTTTCTTGAG-3′; Eomes R, 5′-GGGGTTGAGTCCGTTTATGTT-3′; Brachyury F, 5′-CTGCGCTTCAAGGAGCTAAC-3′; Brachyury R, 5′-CCAGGCCTGACACATTTACC-3′; Mixl1 F, 5′-ACGCAGTGCTTTCCAAACC-3′; Mixl1 R, 5′-CCCGCAAGTGGATGTCTGG-3′; Gata4 F, 5′-CCCTACCCAGCCTACATGG-3′; Gata4 R, 5′-ACATATCGAGATTGGGGTGTCT-3′; Sox17 F, 5′-CGAGCCAAAGCGGAGTCTC-3′; Sox17 R, 5′-TGCCAAGGTCAACGCCTTC-3′; 18S rRNA F, 5′-AGGAATTGACGGAAGGGCACC-3′; and 18S rRNA R, 5′-GTGCAGCCCCGGACATCTAAG-3′.

Western Blot Analyses—Cells were lysed in lysis buffer (50 mM Tris-HCl, pH 7.4, 1% Triton X-100, 0.5% Nonidet P-40, 150 mM NaCl, 1 mM EDTA, 0.1 μM 4-(2-aminoethyl) benzenesulfonyl fluoride, 1 mM Na_3VO_4, 1 mM sodium fluoride, 1 μg/ml aprotinin, 1 μg/ml leupeptin, and 10% glycerol) at 4 °C for 30 min and sonicated (at 10% amplitude for 3 s in a Branson sonifier (Branson, Danbury, CT) equipped with a microtip), followed by centrifugation at 14,000 rpm for 30 min. Proteins were then quantified using BCA assay kit (Pierce). Cell lysates were boiled at 95 °C for 5 min in Laemmli protein sample buffer. The samples were subjected to SDS-PAGE and electrotransferred to nitrocellulose membranes. The membrane was immunoblotted with the anti-c-Myc (Cell Signaling, Danvers, MA), anti-Ahnak (17), anti-OCT4 (H-134; Santa Cruz Biotechnology), anti-SOX2 (Millipore), anti-KLF4 (Santa Cruz Biotechnology), anti-phospho-Smad3 (Cell Signaling, Danvers, MA), or anti-Smad3 (Invitrogen) antibody followed by horseradish peroxidase-conjugated secondary antibody. Bands were visualized by chemiluminescence (Fujifilm LAS-3000; Fujifilm, Stamford, CT). All the Western blot experiments were repeated three times.

Teratoma Formation and Histological Analysis—iPSC (Ahnak$^{-/-}$-iPSC-3F-8) were suspended at 1×10^7 cells/ml in DMEM containing 10% FBS. Nude mice were anesthetized with diethyl ether. Injection of 100 μl of the cell suspension (1×10^6 cells) was applied subcutaneously into the dorsal flank. Four weeks after the injection, tumors were surgically dissected from the mice. The samples were weighed, fixed in PBS containing 4% formaldehyde and embedded in paraffin. The sections were stained with hematoxylin and eosin for histological examination.

Statistics—The data are expressed as the means ± S.D. or ± S.E. of values from three to five independent experiments. Statistical analyses were performed with a two-tailed Student's *t* test. *p* values of <0.05 were considered statistically significant. All Western blots in the figures were representative of three independent experiments.

Results

Mutually Exclusive Expression of Ahnak and c-Myc—We have previously demonstrated that Ahnak plays an inhibitory role in c-Myc expression through TGFβ-Smad3 signaling cascade in epithelial cells (17). To evaluate whether Ahnak regulates c-Myc expression in embryonic fibroblasts, we examined Ahnak knock-out (Ahnak$^{-/-}$) MEF. It was readily seen that c-Myc expression was significantly enhanced in Ahnak$^{-/-}$ MEF compared with that in wild type MEF (Fig. 1*A*). Because c-Myc is expressed in ES cells and is ectopically expressed for efficient iPSC generation, we sought to examine the possible utility of Ahnak in induction of iPSC. We first questioned whether Ahnak expression is dynamically regulated during EB formation from ES cells. Indeed, Ahnak expression was sharply increased during EB formation from ES cells (Fig. 1*B*), whereas expression of Oct4, Nanog, and c-Myc showed changes in the opposite direction. These results are consistent with the idea that the inhibition of Ahnak may provide a favorable condition for maintenance of ES cells in undifferentiated states and possibly induce iPSC in the absence of expressing c-Myc, a proto-oncogene.

Efficient Generation of Ahnak$^{-/-}$ iPSC without Ectopic c-Myc—We sought to check whether ectopic expression of three of the Yamanaka factors (Oct4, Sox2, and Klf4) is suffi-

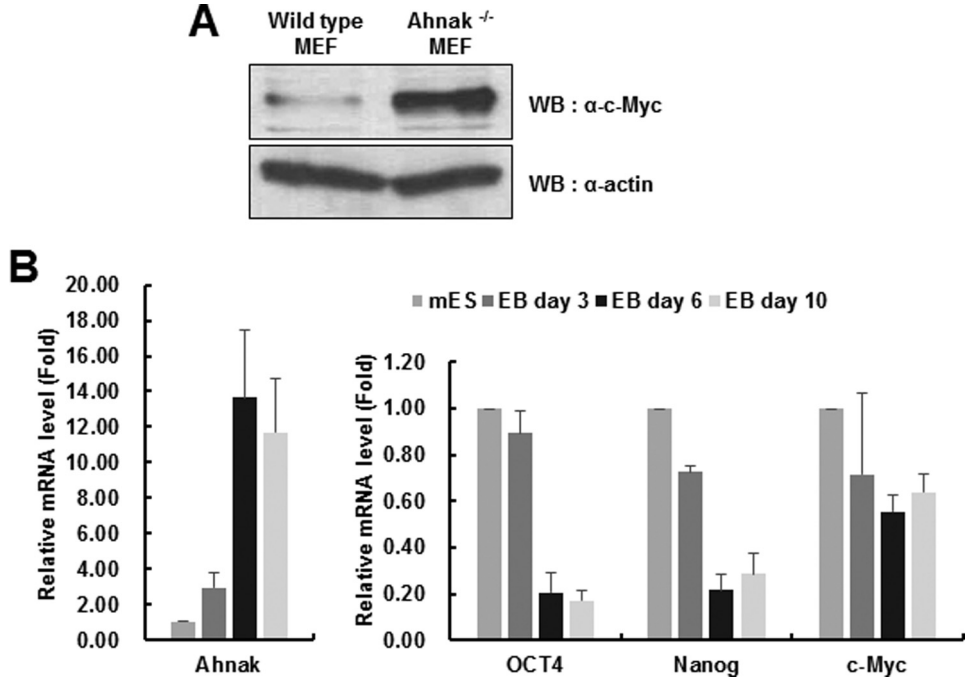

FIGURE 1. **Expression of Ahnak in ES cells and during EB formation.** *A*, expression of c-Myc in wild type and Ahnak$^{-/-}$ MEF. Lysates of MEF cells from wild type and Ahnak$^{-/-}$ mice were subjected to SDS-PAGE and Western blot (*WB*) analysis with antibodies to c-Myc or β-actin. *B*, time course of gene expression in mouse ES (*mES*) cells and ES cell-derived embryoid bodies. Real time PCR analyses of Ahnak and pluripotent gene (OCT4, Nanog, and c-Myc) expression at day 0 (undifferentiated ES cells), day 3, day 6, and day 10 during EB formation by J1 mouse ES cells. Gene expression levels were normalized to the amount of GAPDH mRNA. OCT4 and Nanog represent ES cells-specific genes. *Error bars* signify means ± S.E. from five independent experiments.

cient for efficient iPSC formation in Ahnak$^{-/-}$ MEF without ectopic expression of c-Myc. Indeed, infection of Ahnak$^{-/-}$ MEF with the retroviruses encoding the three factors resulted in significantly increased iPSC generation compared with the level seen with wild type MEF (Fig. 2, *A* and *B*). This may have resulted from the fact that c-Myc expression was increased in Ahnak deficient cells. To evaluate the effect of c-Myc on iPSC generation, c-Myc gene was transfected in wild type MEF cells in various doses along with the other three transcription factors. Efficiency in iPSC generation clearly increased in a c-Myc dose-dependent manner (Fig. 2, *C* and *D*).

We next questioned whether knockdown of Ahnak has similar effects on iPSC generation. A miR-shRNA specific to Ahnak was constructed for retroviral delivery via infection of wild type MEF cells. We found that knockdown of Ahnak expression resulted in a sharp up-regulation of c-Myc expression as we saw in Ahnak$^{-/-}$ cells (Fig. 3*A*). Consistently, infection of wild type MEF cells with retrovirus expressing Ahnak-specific miR-shRNA led to a significantly increased level of iPSC generation compared with infection of control miR-shRNA retrovirus (Fig. 3, *B* and *C*). The difference was seen either with all four Yamanaka factors or with three of them (*i.e.* without c-Myc) consistent with the c-Myc dose-dependent efficiency of iPSC generation. We next examined whether knockdown of Ahnak has similar effects in human fibroblasts. As was the case in MEF, we saw clear increase in c-Myc protein level and a concomitant increase in AP-positive colonies (Fig. 3, *D* and *E*), indicating that the Ahnak regulation can be applied in human iPSC generation as well.

Characterization and Development of iPSC—We characterized the expression of the Yamanaka factors (Oct4, Sox2, Klf4, and c-Myc) in iPSC generated from wild type (WT-iPSC-4F-#5, -#6, -#16, -#17, -#19; WT-iPSC-3F-#1, -#3, -#4, -#6, -#8) and Ahnak$^{-/-}$ MEF (Ahnak$^{-/-}$-iPSC-4F-#5, -#29, -#31, -#38, -#46; Ahnak$^{-/-}$-iPSC-3F-#3, -#4, -#6, -#7, -#8) cells after infection with four (4F) or three (3F; *i.e.* without c-Myc) of the Yamanaka factors. We found that the combined expression level of endogenous (Fig. 4*A*, *open bars*) and transgenic transcripts (Fig. 4*A*, *solid bars*) for each of the four factors was higher in the four different iPSC (five independent cell lines of each WT-iPSC-4F; Ahnak$^{-/-}$-iPSC-4F; WT-iPSC-3F; Ahnak$^{-/-}$-iPSC-3F) tested than that in undifferentiated J1 ES or uninfected MEF cells. All four iPSC lines derived from MEF expressed significant levels of endogenous Oct4, Sox2, Klf4, and c-Myc, consistent with all cell lines ultimately achieving sustainable stemness. Moreover, we investigated the expression of Oct4, Sox2, and SSEA1 of the four different iPSC lines at the protein level via immunocytochemical analyses. Expression of Oct4 and Sox2 was readily observed in the nuclei of iPSC, as well as mouse embryonic J1 cells (Fig. 4*B*). SSEA1 was also detected in cell surface of all iPSC lines and J1 cells (Fig. 4*B*). These results indicate that the four different iPSC have been successfully endowed with properties of pluripotent stem cells (Fig. 4*B*). We next examined the molecular connection between Smad3 phosphorylation as an indication of TGFβ activation and c-Myc expression as the downstream event during iPSC generation. Wild type or Ahnak$^{-/-}$ MEF cells were transduced with all four Yamanaka factors (4F; Oct4, Sox2, Klf4, and c-Myc) or three factors (3F; Oct4, Sox2, and Klf4), and then these cells were tested for the levels of SMAD3 phosphorylation and c-Myc expression during iPSC generation (WT-4F; Ahnak$^{-/-}$-4F; WT-3F; Ahnak$^{-/-}$-3F). As expected, infection of Ahnak$^{-/-}$ MEF cells with 4F or 3F resulted in significantly increased c-Myc expression, com-

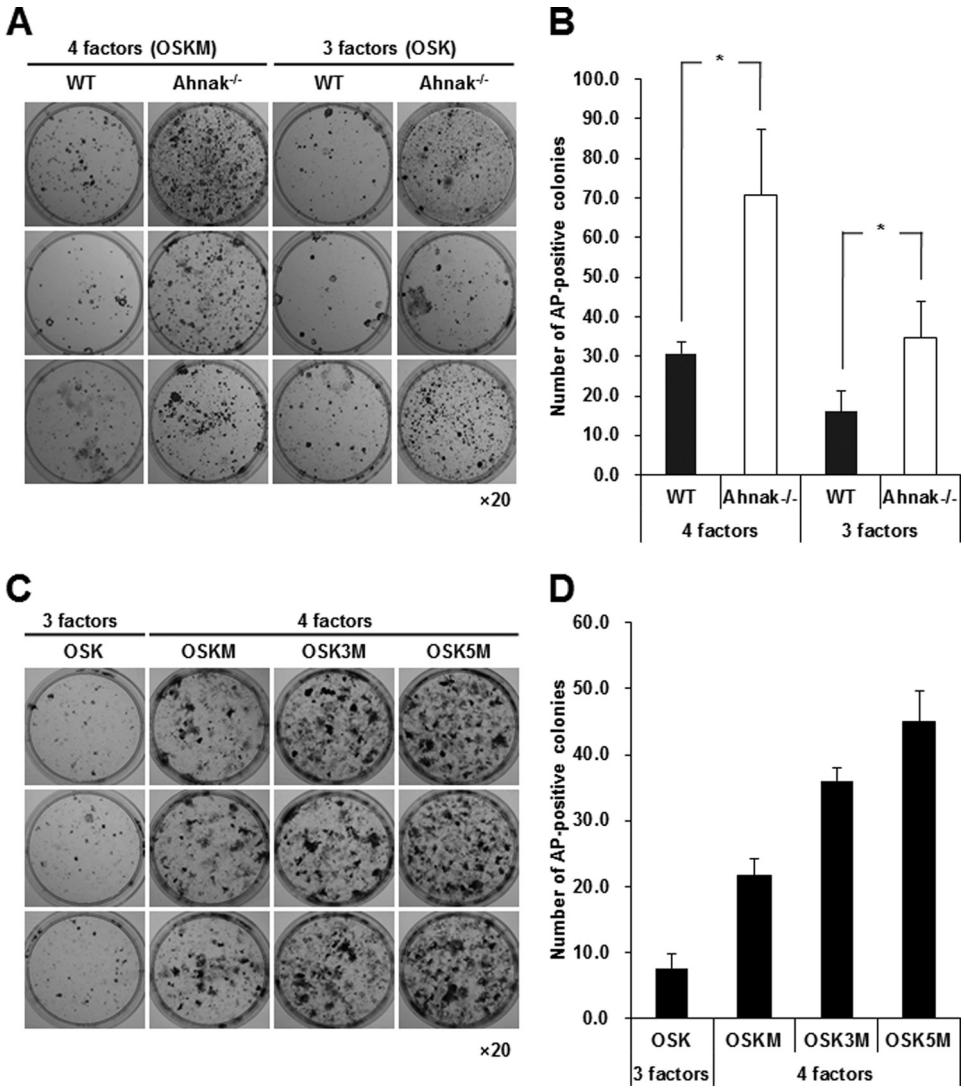

FIGURE 2. **Efficient reprogramming of Ahnak$^{-/-}$ MEF without c-Myc.** *A*, alkaline phosphatase staining of wild type and Ahnak$^{-/-}$ iPSC generated with four (OSKM) or three Yamanaka factors (OSK). Wild type and Ahnak$^{-/-}$ MEF (1.5×10^5) were transduced with a mixture of the retroviral medium containing four factors (OCT4, SOX2, KLF4, and c-Myc) or three factors (OCT4, SOX2, and KLF4). Alkaline phosphatase-positive colonies were counted on day 18. *B*, the number of alkaline phosphatase-positive colonies from wild type and Ahnak$^{-/-}$ iPSC 18 days after retroviral transduction. *Error bars* represent means ± S.D. from three independent experiments. *, $p < 0.05$. *C*, increased efficiency of iPSC generation by c-Myc expression in a dose-dependent manner. Reprogrammed cells stained for Alkaline phosphatase. Wild type MEF (1.5×10^5) were transducted with a mixture of the retroviral medium containing just the three factors (OCT4, SOX2, and KLF4) or in addition with varying doses of c-Myc virus. Alkaline phosphatase-positive colonies were counted on day 18. *D*, the number of Alkaline phosphatase-positive colonies. *Error bars* represent means ± S.D. from three independent experiments.

pared with wild type MEF cells infected by 4F or 3F (Fig. 4*C*). However, phosphorylation of Smad3 in Ahnak$^{-/-}$ MEF infected with 3F was only slightly lower than that in WT MEF infected with 3F (Fig. 4*C*). This implies that the lack of phospho-Smad3 does not contribute much to c-Myc expression during iPSC generation. It follows that the initial level of c-Myc in Ahnak$^{-/-}$ MEF likely plays an important role in the contribution of iPSC generation.

To further examine the pluripotency of iPSC from wild type and Ahnak$^{-/-}$ MEF cells generated either with four or three of Yamanaka factors, we analyzed the expression of representative markers for endoderm, mesoderm, and ectoderm after differentiation. The iPSC were induced to form EBs and then examined by immunocytochemistry with antibodies to βIII tubulin (for ectoderm), smooth muscle actin (for mesoderm), and α-fetoprotein (for endoderm). We found that all three markers were expressed in WT-iPSC-4F-#19 and Ahnak$^{-/-}$-iPSC-4F-#31, as well as in WT-iPSC-3F-#6 and Ahnak$^{-/-}$-iPSC-3F-#8, indicating pluripotency of the four different iPSC lines we generated (Fig. 5*A*). To evaluate transcriptional expression of three germ layer marker genes, expression levels of ectoderm marker genes (FGF5 and Nestin), mesoderm marker genes (Eomes, Brachyury, and Mixl1), and endoderm marker genes (Gata4 and Sox17) during EB formation (up to day 10) were investigated. Expression levels of representative marker genes for the three germ layers during EB differentiation of four established cell lines were shown to be similar to those seen with mES (Fig. 5*B*).

Finally, we tested whether Ahnak$^{-/-}$-iPSC-3F-#8 cells can form teratoma. To this end, the cells were injected into immunodeficient SCID/beige mice, and induced nodules were histologically examined for the presence of all three embryonic germ layers (ectoderm, mesoderm, and endoderm). Indeed we found

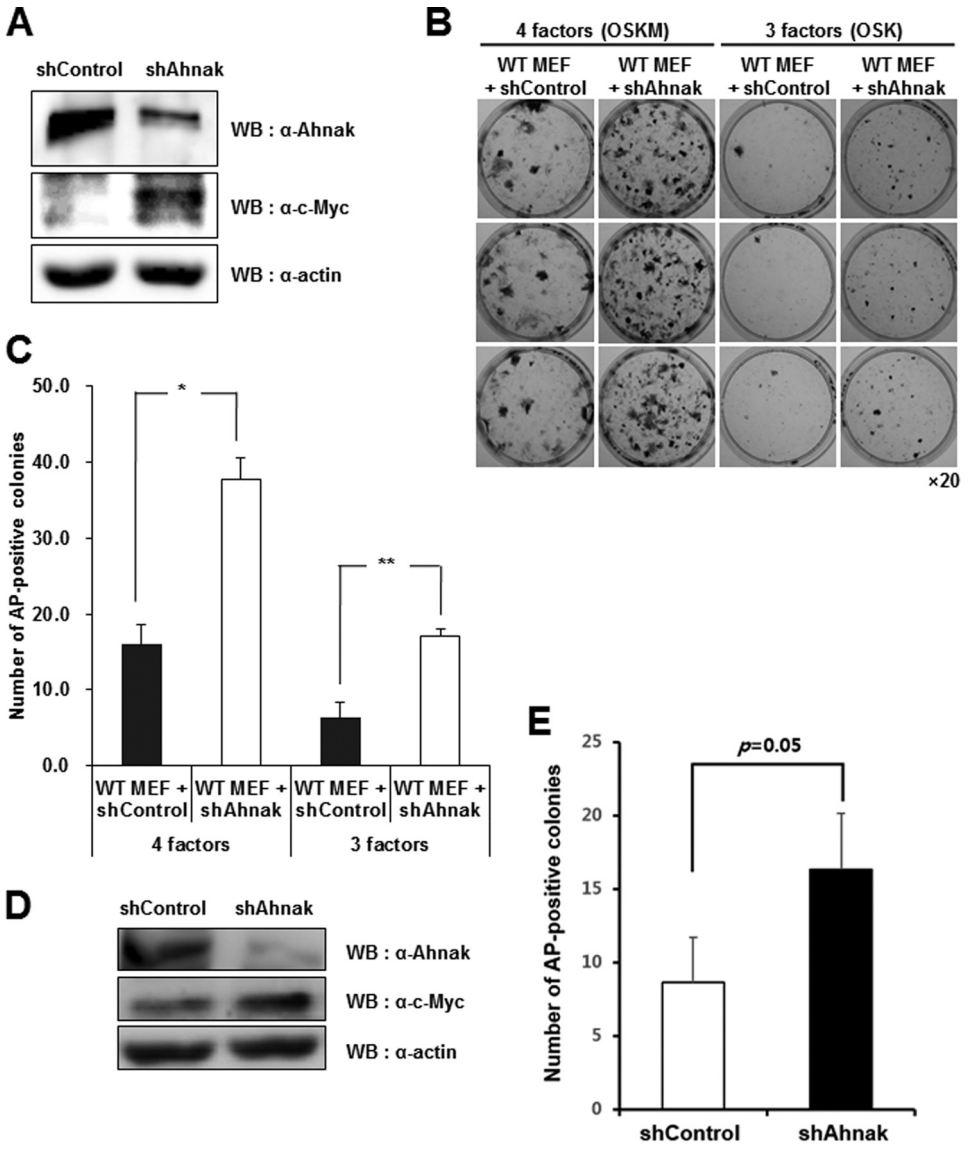

FIGURE 3. **Increased efficiency of iPSC generation by down-regulation of Ahnak expression.** *A*, expression of c-Myc in Ahnak knockdown MEF. Lysates of MEF cells were subjected to SDS-PAGE and Western blot (*WB*) analysis with antibodies to Ahnak, c-Myc, and β-actin. *B*, alkaline phosphatase staining of wild type iPSC generated by four factors (OSKM) or three factors (OSK) in combination with scrambled control shRNA or Ahnak-specific shRNA. Wild type MEF (1.5×10^5) were transduced with a mixture of the retroviral medium containing four factors (OCT4, SOX2, KLF4, and c-Myc) and scrambled shRNA, four factors (OSKM) and Ahnak-specific shRNA, three factors (OCT4, SOX2, and KLF4) and scrambled shRNA, or three factors (OSK) and Ahnak-specific shRNA. Alkaline phosphatase-positive colonies were counted on day 18. *C*, the number of alkaline phosphatase-positive colonies counted 18 days after retroviral transduction. *Error bars* represent means ± S.D. from three independent experiments. *, $p < 0.001$; **, $p < 0.005$. *D*, expression of c-Myc in Ahnak knockdown HFF cells. Lysates of HFF cells were subjected to SDS-PAGE and Western blot analysis with antibodies to Ahnak, c-Myc, and β-actin. *E*, the number of alkaline phosphatase-positive colonies from HEF cells counted 14 days after retroviral transduction. *Error bars* represent means ± S.D. from three independent experiments ($p = 0.05$).

that neural-like tissues (Fig. 6, *arrowheads* in *panels a*, *b*, *e*, and *f*) and epidermis (Fig. 6, *arrowheads* in *panels c*, *d*, *g*, and *h*) representing ectoderm, cartilage (Fig. 6, *arrowheads* in *panels i*, *j*, *m*, and *n*) and muscle tissues (Fig. 6, *arrowheads* in *panels k*, *l*, *o*, and *p*) representing mesoderm, and gut-like epithelium (Fig. 6, *arrowheads* in *panels q–x*) representing endoderm in nodules from seven of eight mice. Together with results from examination of EB, these data indicate that Ahnak$^{-/-}$-iPSC-3F-#8 cells are *bona fide* pluripotent stem cells.

Discussion

Because the four transcription factors Oct4, Sox2, Klf4, and c-Myc have been shown to activate reprogramming of somatic cells to pluripotent stem cells, efforts have been continually made to improve the efficiency of the induction and safety of the iPSC application. The chief safety concern for iPSC is the potential for tumorigenesis. In particular, the inclusion of c-Myc, a powerful proto-oncogene, in the induction process has represented the major hurdle for medical application of these cells (2). Specifically, it has been reported that tumors from iPSC often show reactivation of exogenous c-Myc (2).

Multiple studies have reported successful iPSC generation without exogenous c-Myc. For example, generation of human iPSC has been successfully carried out with the combination of Oct4, Sox2, Nanog, and Lin28 (22). Also, N-Myc or L-Myc can replace c-Myc for the generation of iPSC (18, 19). Inclusion of

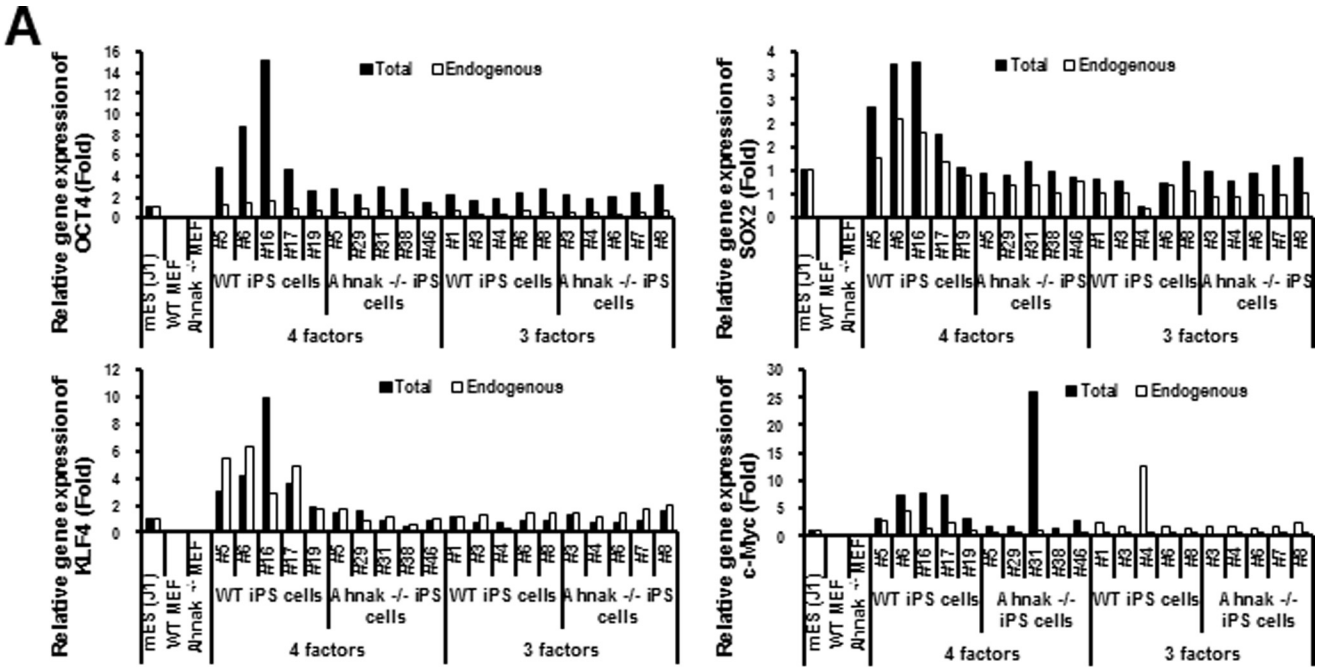
A
Relative gene expression of OCT4 (Fold)
Relative gene expression of SOX2 (Fold)
Relative gene expression of KLF4 (Fold)
Relative gene expression of c-Myc (Fold)
Total
Endogenous
mES (J1)
WT MEF
Ahnak -/- MEF
WT iPS cells
Ahnak -/- iPS cells
4 factors
3 factors

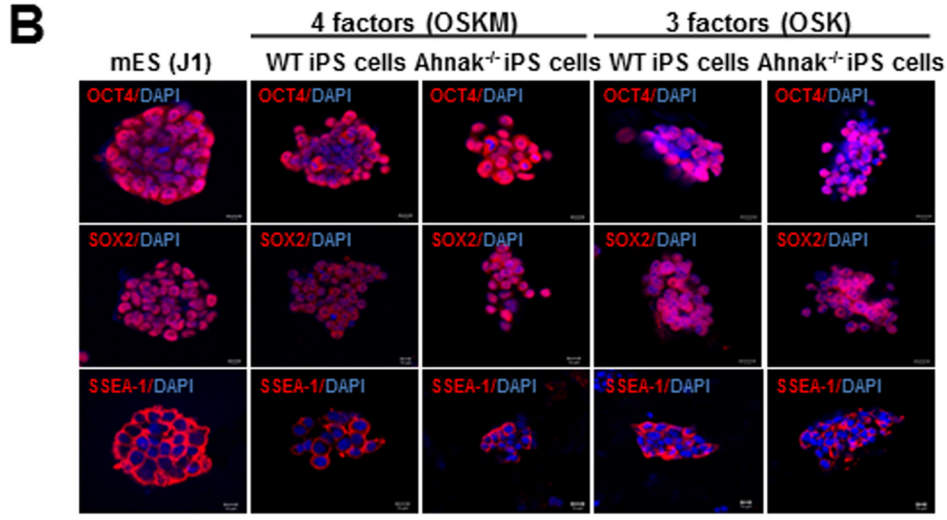
B
4 factors (OSKM)
3 factors (OSK)
mES (J1)
WT iPS cells
Ahnak-/- iPS cells
OCT4/DAPI
SOX2/DAPI
SSEA-1/DAPI

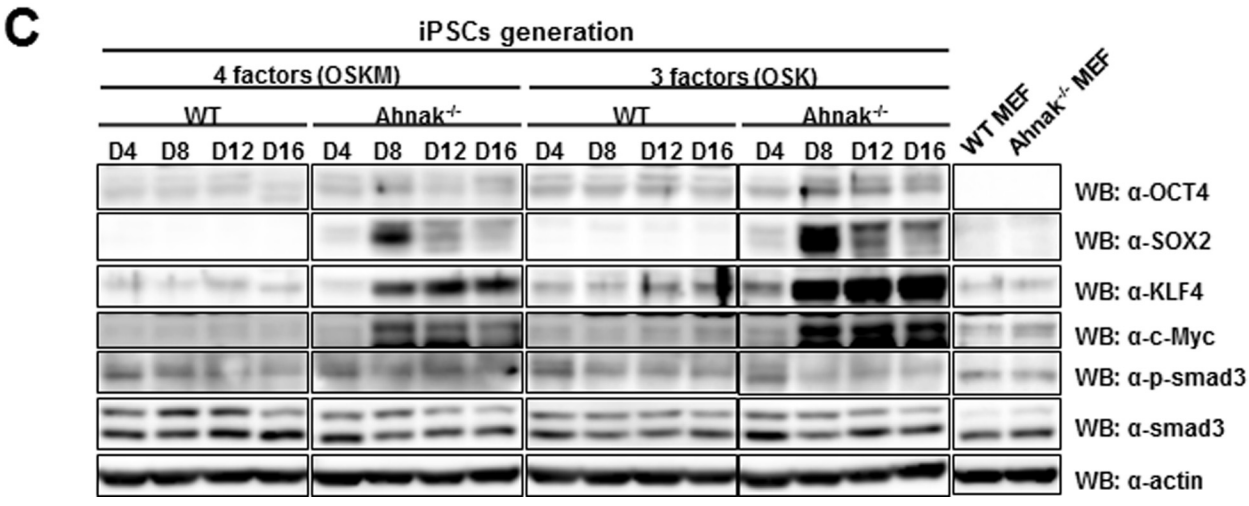
C
iPSCs generation
4 factors (OSKM)
3 factors (OSK)
WT
Ahnak-/-
D4 D8 D12 D16
WT MEF
Ahnak-/- MEF
WB: α-OCT4
WB: α-SOX2
WB: α-KLF4
WB: α-c-Myc
WB: α-p-smad3
WB: α-smad3
WB: α-actin

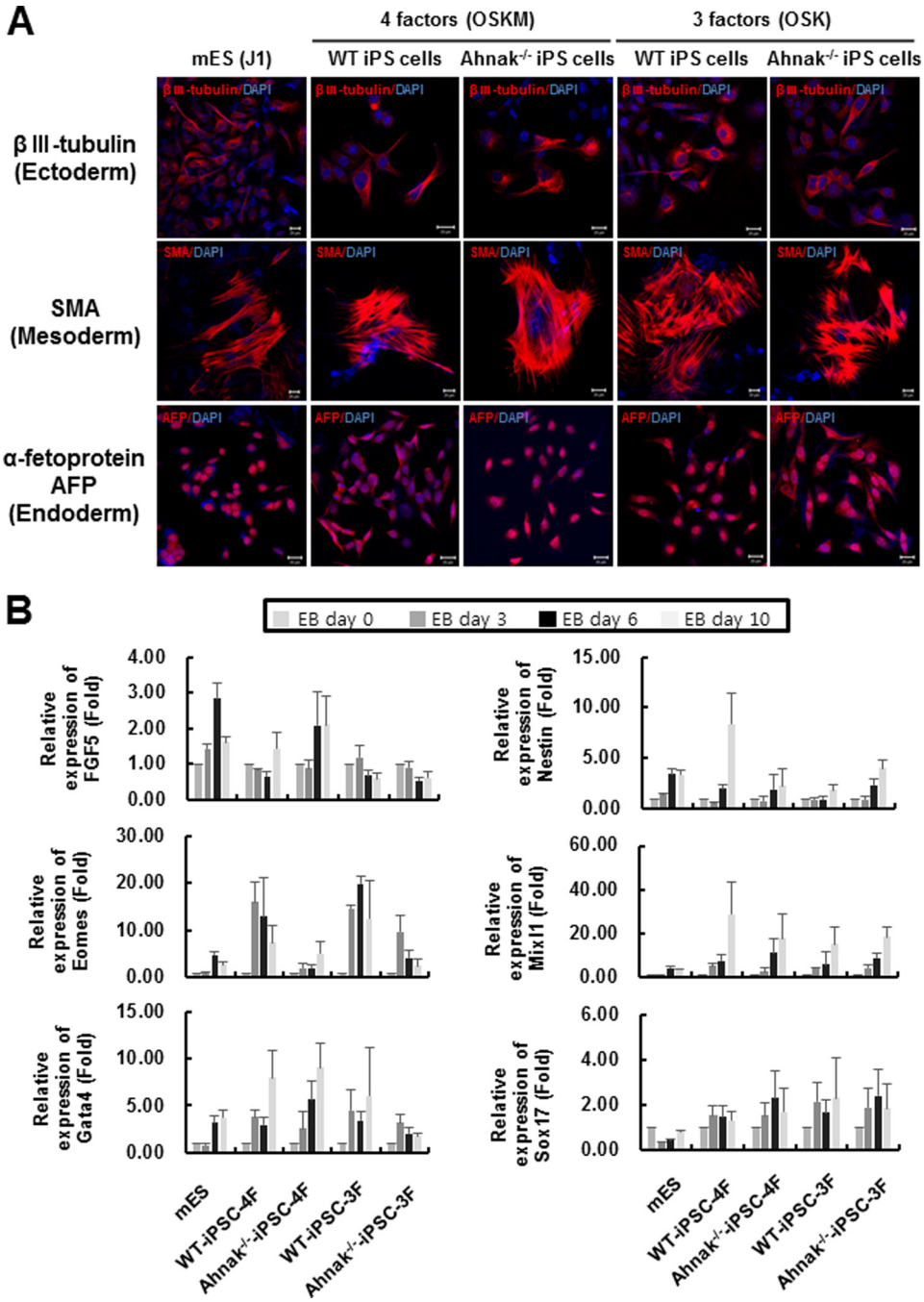

FIGURE 5. **Differentiation of iPSC derived from wild type and Ahnak$^{-/-}$ MEF.** *A*, *in vitro* differentiation of wild type and Ahnak$^{-/-}$ iPSC generated with four (OSKM) or three factors (OSK). Immunofluorescence staining showing the expression of the three germ layer marker genes, βIII-tubulin (for ectoderm), smooth muscle actin (*SMA*; for mesoderm), and α-fetoprotein (for endoderm) in the differentiated mouse ES cells, wild type MEF-derived iPSC, and Ahnak$^{-/-}$ MEF-derived iPSC. Nuclei are stained with DAPI (*blue*). A representative image is shown for each combination of cell type and marker. *Scale bar*, 20 μm. *B*, time-dependent expression of three germ layer marker genes in mouse ES cells or four different established iPSC (WT-iPSC-4F; Ahnak$^{-/-}$-iPSC-4F; WT-iPSC-3F; Ahnak$^{-/-}$-iPSC-3F). Expression levels of ectoderm markers (FGF5, Nestin), mesoendodermal marker (Eomes), mesoderm marker (Brachyury, Mixl1), and endoderm markers (Gata4, Sox17) were investigated during EB formation (days 0, 3, 6, and 10) in mouse ES cells and four different established iPSC. Gene expression levels were normalized to the amount of GAPDH mRNA. *Error bars* signify means ± S.E. from three independent experiments.

FIGURE 4. **Characterization of iPSC derived from wild type and Ahnak$^{-/-}$ MEF.** *A*, confirmation of pluripotency marker gene expression in iPSC. Quantitative real time PCR analyses of OCT4, SOX2, KLF4, and c-Myc expression in mouse ES cells, MEF cells, wild type MEF-derived iPSC, and Ahnak$^{-/-}$ MEF-derived iPSC. Gene expression levels were normalized to the amount of 18S rRNA. "Endogenous" means that oligonucleotide primers located in the 5′- and 3′-untranslated regions were used to measure the expression of the endogenous genes only. "Total" means that primers in coding regions were used to measure the expression of both the endogenous and viral transcripts. *B*, immunofluorescence staining showing the expression of the pluripotency marker proteins OCT4, SOX2, and SSEA1 (*red*) in mouse ES cells, wild type MEF-derived iPSC, and Ahnak$^{-/-}$ MEF-derived iPSC. Both types of iPSC (*i.e.* those generated with four factors and those with three factors) were examined. Nuclei are counterstained with DAPI (*blue*). A representative image is shown for each combination of cell type and marker. *Scale bar*, 10 μm. *C*, expression of the OCT4, SOX2, KLF4, c-Myc, and phosphorylation level of Smad3 during iPSC generation. Wild type and Ahnak$^{-/-}$ MEF were infected with retrovirus containing four factors (OCT4, SOX2, KLF4, and c-Myc) or three factors (OCT4, SOX2, and KLF4) and then subjected to Western blot (*WB*) analysis with antibodies against OCT4, SOX2, KLF4, c-Myc, phospho-Smad3, Smad3, and actin.

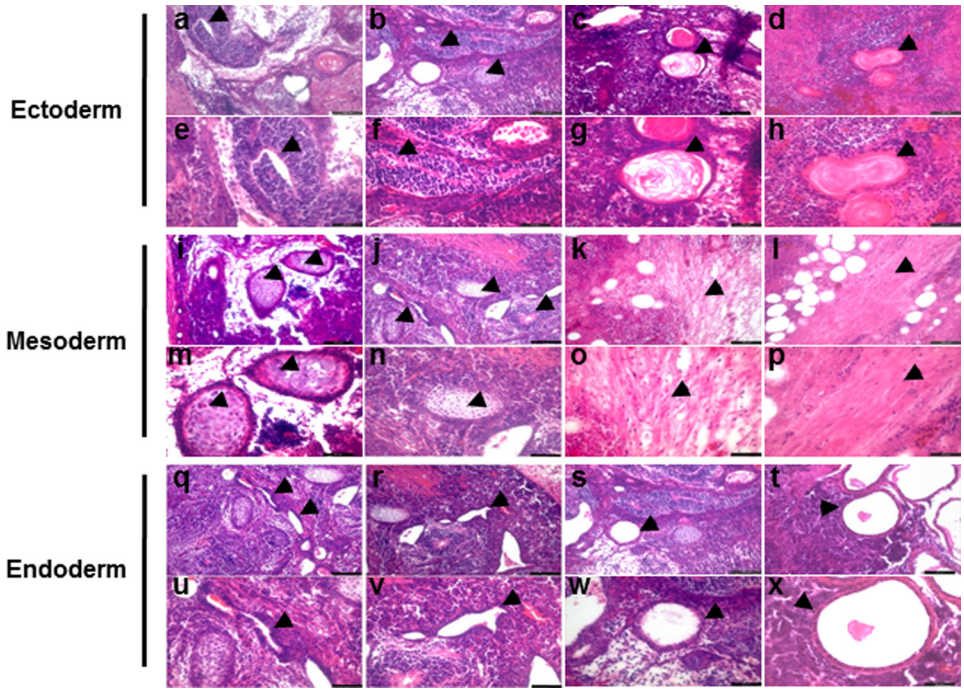

FIGURE 6. **Teratoma formation by iPSC generated from Ahnak$^{-/-}$ MEF.** Histology of teratomas formed after injection of iPSC from Ahnak$^{-/-}$ MEF with three factors into immunodeficient SCID/beige mice. The teratoma contained derivatives of all three embryonic germ layers. *Panels a–d*, *i–l*, and *q–t*, low magnification (100×; *bar*, 100 μm) views of the teratoma tissue sections. *Panels e–h*, *m–p*, and *u–x*, high magnification (200×; *bar*, 50 μm) views of *panels a–d*, *i–l*, and *q–t*, respectively. *Panels a*, *b*, *e*, and *f*, *arrowheads* point to neural-like tissues. *Panels c*, *d*, *g*, and *h*, *arrowheads* point to epidermis-like tissues. *Panels i*, *j*, *m*, and *n*, *arrowheads* point to cartilage-like tissues. *Panels k*, *l*, *o*, and *p*, *arrowheads* point to muscle-like tissues. *Panels q–x*, *arrowheads* point to gut-like epithelium. All images were obtained from formalin-fixed and paraffin-embedded teratoma sections stained with hematoxylin and eosin.

UTF1 and siRNA for p53, as well as expression of poly(ADP-ribose) polymerase 1, also could replace c-Myc and lead to efficient iPSC generation (23, 24). Still, studies involving direct comparisons demonstrated that efficiency of iPSC generation decreases in the absence of c-Myc (18–20, 25).

Ahnak, a scaffold protein, binds to R-Smad, potentiates TGFβ-mediated cell signaling, and thereby induces down-regulation of c-Myc expression (13). Given that Ahnak expression is increased during the differentiation of ES cells to EB, whereas Oct4 and Nanog, representative markers of iPSC, are down-regulated, it was possible to hypothesize that Ahnak is a gene with an anti-stemness property. Our success in improving the efficiency in the absence of ectopic expression of c-Myc via down-regulating Ahnak suggests another possible way of generating safer iPSC.

We have in fact found multiple reports indicating that inhibition of TGF-β signaling promotes induction of pluripotency (26–29). This is consistent with our results that at least during the initial phase of induction, TGF-β signaling should be inhibited rather than enhanced for an efficient induction of pluripotency. It is likely that some TGF-β signaling is in taking place in ES or iPSC given that some p-Smad3 is detected (Fig. 4*C*). However, it is clear that the signaling is not strong enough to turn off c-Myc expression. It could be in this context that the p-Smad3 level we observed can be interpreted (Fig. 4*C*). In fact, given that Ahnak$^{-/-}$ mice are viable and that p-Smad3 is detected in Ahnak$^{-/-}$ cells, we could safely conclude that Ahnak-independent mechanism can mediate a certain level of TGF-β signaling, and this is not mutually exclusive with c-Myc expression. Alternatively, it is also possible that once iPSC is established, c-Myc expression attains a measure of independence from TGF-β signaling, which allows coexistence of TGF-β signaling and c-Myc expression in iPSC.

Importantly, the iPSC (Ahnak$^{-/-}$-iPSC-3F-#8) generated from Ahnak$^{-/-}$ MEF without c-Myc could differentiate into all three germ layers *in vitro* and could generate teratoma efficiently *in vivo*. Although Ahnak plays an important role in many biological processes, deficiency of Ahnak apparently did not affect manifestation of pluripotency. That transient knockdown expression of Ahnak also improved iPSC generation without c-Myc implies the potential for a broad application of Ahnak regulation in generation and differentiation of iPSC. With the detailed molecular mechanism by which Ahnak regulates c-Myc in various context elucidated, Ahnak and molecular components of pathways Ahnak regulates could develop into important targets in regulating generation of safe iPSC with efficiency.

Author Contributions—Y. S. B. and J. K. conceived and coordinated the study and wrote the manuscript. H. J. L. designed, performed, and analyzed the experiments shown in Figs. 1, 2, 4, and 5. J. K., S. A. L., and M. R. L. designed, performed, and analyzed the experiments shown in Fig. 3. C.-H. P. and K.-S. K. designed, performed, and analyzed the experiments shown in Fig. 6. All authors reviewed the results and approved the final version of the manuscript.

References

1. Takahashi, K., and Yamanaka, S. (2006) Induction of pluripotent stem cells from mouse embryonic and adult fibroblast cultures by defined factors. *Cell* **126,** 663–676

2. Okita, K., Ichisaka, T., and Yamanaka, S. (2007) Generation of germline-competent induced pluripotent stem cells. *Nature* **448,** 313–317
3. Wernig, M., Meissner, A., Foreman, R., Brambrink, T., Ku, M., Hochedlinger, K., Bernstein, B. E., and Jaenisch, R. (2007) *In vitro* reprogramming of fibroblasts into a pluripotent ES-cell-like state. *Nature* **448,** 318–324
4. Lowry, W. E., Richter, L., Yachechko, R., Pyle, A. D., Tchieu, J., Sridharan, R., Clark, A. T., and Plath, K. (2008) Generation of human induced pluripotent stem cells from dermal fibroblasts. *Proc. Natl. Acad. Sci. U.S.A.* **105,** 2883–2888
5. Park, I. H., Zhao, R., West, J. A., Yabuuchi, A., Huo, H., Ince, T. A., Lerou, P. H., Lensch, M. W., and Daley, G. Q. (2008) Reprogramming of human somatic cells to pluripotency with defined factors. *Nature* **451,** 141–146
6. Rosner, M. H., Vigano, M. A., Ozato, K., Timmons, P. M., Poirier, F., Rigby, P. W., and Staudt, L. M. (1990) A POU-domain transcription factor in early stem cells and germ cells of the mammalian embryo. *Nature* **345,** 686–692
7. Pan, G. J., Chang, Z. Y., Schöler, H. R., and Pei, D. (2002) Stem cell pluripotency and transcription factor Oct4. *Cell Res.* **12,** 321–329
8. Avilion, A. A., Nicolis, S. K., Pevny, L. H., Perez, L., Vivian, N., and Lovell-Badge, R. (2003) Multipotent cell lineages in early mouse development depend on SOX2 function. *Genes Dev.* **17,** 126–140
9. Nandan, M. O., and Yang, V. W. (2009) The role of Kruppel-like factors in the reprogramming of somatic cells to induced pluripotent stem cells. *Histol. Histopathol.* **24,** 1343–1355
10. Tetreault, M. P., Yang, Y., and Katz, J. P. (2013) Kruppel-like factors in cancer. *Nat. Rev. Cancer* **13,** 701–713
11. Adhikary, S., and Eilers, M. (2005) Transcriptional regulation and transformation by MYC proteins. *Nat. Rev. Mol. Cell Biol.* **6,** 635–645
12. Cartwright, P., McLean, C., Sheppard, A., Rivett, D., Jones, K., and Dalton, S. (2005) LIF/STAT3 controls ES cell self-renewal and pluripotency by a Myc-dependent mechanism. *Development* **132,** 885–896
13. Sekiya, F., Bae, Y. S., Jhon, D. Y., Hwang, S. C., and Rhee, S. G. (1999) AHNAK, a protein that binds and activates phospholipase C-γ1 in the presence of arachidonic acid. *J. Biol. Chem.* **274,** 13900–13907
14. Lee, I. H., You, J. O., Ha, K. S., Bae, D. S., Suh, P. G., Rhee, S. G., and Bae, Y. S. (2004) AHNAK-mediated activation of phospholipase C-γ1 through protein kinase C. *J. Biol. Chem.* **279,** 26645–26653
15. Lee, I. H., Lim, H. J., Yoon, S., Seong, J. K., Bae, D. S., Rhee, S. G., and Bae, Y. S. (2008) Ahnak protein activates protein kinase C (PKC) through dissociation of the PKC-protein phosphatase 2A complex. *J. Biol. Chem.* **283,** 6312–6320
16. Lim, H. J., Kang, D. H., Lim, J. M., Kang, D. M., Seong, J. K., Kang, S. W., and Bae, Y. S. (2013) Function of Ahnak protein in aortic smooth muscle cell migration through Rac activation. *Cardiovasc. Res.* **97,** 302–310
17. Lee, I. H., Sohn, M., Lim, H. J., Yoon, S., Oh, H., Shin, S., Shin, J. H., Oh, S. H., Kim, J., Lee, D. K., Noh, D. Y., Bae, D. S., Seong, J. K., and Bae, Y. S. (2014) Ahnak functions as a tumor suppressor via modulation of TGF β/Smad signaling pathway. *Oncogene* **33,** 4675–4684
18. Nakagawa, M., Koyanagi, M., Tanabe, K., Takahashi, K., Ichisaka, T., Aoi, T., Okita, K., Mochiduki, Y., Takizawa, N., and Yamanaka, S. (2008) Generation of induced pluripotent stem cells without Myc from mouse and human fibroblasts. *Nat. Biotechnol.* **26,** 101–106
19. Wernig, M., Meissner, A., Cassady, J. P., and Jaenisch, R. (2008) c-Myc is dispensable for direct reprogramming of mouse fibroblasts. *Cell Stem Cell* **2,** 10–12
20. Robinton, D. A., and Daley, G. Q. (2012) The promise of induced pluripotent stem cells in research and therapy. *Nature* **481,** 295–305
21. Choi, M. K., Seong, I., Kang, S. A., and Kim, J. (2014) Down-regulation of Sox11 is required for efficient osteogenic differentiation of adipose-derived stem cells. *Mol. Cells* **37,** 337–344
22. Yu, J., Vodyanik, M. A., Smuga-Otto, K., Antosiewicz-Bourget, J., Frane, J. L., Tian, S., Nie, J., Jonsdottir, G. A., Ruotti, V., Stewart, R., Slukvin, I. I., and Thomson, J. A. (2007) Induced pluripotent stem cell lines derived from human somatic cells. *Science* **318,** 1917–1920
23. Zhao, Y., Yin, X., Qin, H., Zhu, F., Liu, H., Yang, W., Zhang, Q., Xiang, C., Hou, P., Song, Z., Liu, Y., Yong, J., Zhang, P., Cai, J., Liu, M., Li, H., Li, Y., Qu, X., Cui, K., Zhang, W., Xiang, T., Wu, Y., Zhao, Y., Liu, C., Yu, C., Yuan, K., Lou, J., Ding, M., and Deng, H. (2008) Two supporting factors greatly improve the efficiency of human iPSC generation. *Cell Stem Cell* **3,** 475–479
24. Chiou, S. H., Jiang, B. H., Yu, Y. L., Chou, S. J., Tsai, P. H., Chang, W. C., Chen, L. K., Chen, L. H., Chien, Y., and Chiou, G. Y. (2013) Poly(ADP-ribose) polymerase 1 regulates nuclear reprogramming and promotes iPSC generation without c-Myc. *J. Exp. Med.* **210,** 85–98
25. Theunissen, T. W., and Jaenisch, R. (2014) Molecular control of induced pluripotency. *Cell Stem Cell* **14,** 720–734
26. Vrbsky, J., Tereh, T., Kyrylenko, S., Dvorak, P., and Krejci, L. (2015) MEK and TGF-β inhibition promotes reprogramming without the use of transcription factor. *PLoS One* **10,** e0127739
27. Tan, F., Qian, C., Tang, K., Abd-Allah, S. M., and Jing, N. (2015) Inhibition of transforming growth factor β (TGF-β) signaling can substitute for Oct4 protein in reprogramming and maintain pluripotency. *J. Biol. Chem.* **290,** 4500–4511
28. Dai, P., Harada, Y., Miyachi, H., Tanaka, H., Kitano, S., Adachi, T., Suzuki, T., Hino, H., and Takamatsu, T. (2014) Combining TGF-β signal inhibition and connexin43 silencing for iPSC induction from mouse cardiomyocytes. *Sci. Rep.* **4,** 7323
29. Zhou, J., Su, P., Li, D., Tsang, S., Duan, E., and Wang, F. (2010) High-efficiency induction of neural conversion in human ESCs and human induced pluripotent stem cells with a single chemical inhibitor of transforming growth factor β superfamily receptors. *Stem Cells* **28,** 1741–1750